DALTON

Dissolving alkali metals in zeolites: genesis of the perfect cluster crystal †

Lee J. Woodall,[a] Paul A. Anderson,[a] A. Robert Armstrong[b] and Peter P. Edwards*[,a]

[a] *School of Chemistry, University of Birmingham, Edgbaston, Birmingham B15 2TT, UK*
[b] *School of Chemistry, The University, St. Andrews, Fife KY16 9ST, UK*

The interaction of alkali metals with dehydrated zeolites Y and A leads, in a process which bears many similarities to the dissolution of those metals in non-aqueous liquid solvemts, to the formation of inclusion compounds which may be regarded as ordered arrays of closely spaced clusters, and whose properties are dependent on interactions between the clusters. A combined analysis of electron spin resonance, magnetic susceptibility and powder neutron diffraction results enabled us to follow in detail the chemistry behind the formation of sodium- and potassium-based 'cluster crystals' in zeolites Y and A respectively.

The regular intracrystalline channels and cavities of a dehydrated zeolite (Fig. 1) constitute a periodic array of cation-lined nanoscale spaces into which the controlled and continuous doping of 'excess electrons' is possible through reaction with alkali-metal vapour.[1] Incoming metal atoms are ionized by the intense electric fields within the zeolite releasing electrons to interact with the zeolite cations. The unique opportunity to control continuously and precisely the excess of electron density over a wide range, within tightly confined dimensions and without any significant structural change in the framework, has placed alkali-metal-loaded zeolites at the forefront of current research into materials design.[2–6] Of particular interest is the evolution of electron delocalization in systems close to a composition-dependent insulator-to-metal transition, which is of enormous theoretical *and* practical importance as it underpins attempts to design solids with specific electronic and magnetic properties.[1,7–12]

To understand the chemistry behind the formation of these important materials it is appropriate to consider the zeolite as a solid polar solvent, and the process of dissolving the alkali metals has many elements of similarity, both conceptually and phenomenologically, to the dissolution of alkali metals in non-aqueous liquid solvents.[1,11,13] Although the comparison with metal–liquid solutions provides a remarkably robust conceptual framework for rationalizing the properties of a wide range of metal–zeolite compounds, the precise details of the nature of the species formed remain dependent on the zeolite structure, the exchangeable cations and, of course, the metal used.[13] In consequence of the rich variety of observations associated with this class of compounds, a number of defining concepts, each with its own particular merits, have been developed. Examples include the 'cationic/metallic continua' in zeolite A described by Seff and co-workers,[14,15] and the idea of alkali-metal-loaded zeolites as 'inorganic electrides'.[8,13,16] Materials based on zeolites containing one-dimensional channels have also been highlighted as potential 'quantum wire arrays'.[4,6,12]

In the case of zeolites possessed of a cage structure, almost all workers have found it convenient to discuss their compounds in terms of alkali-metal clusters confined within the various cages. This is particularly true of zeolites containing the sodalite cage structural unit (zeolites X, Y and A, see Fig. 1), which have been shown by ESR and structural studies to play host to a range of caesium, rubidium, potassium and sodium clusters.[17–22] While the individual clusters are themselves of considerable interest, it is their preparation within the regular periodic pore space of a zeolite that can uniquely provide us with an ordered array of closely spaced clusters, the so-called 'cluster crystal'.[2,23] The properties of such arrays are strongly influenced by interactions between the clusters, which are in turn dependent on the geometry imposed by the zeolite framework. In this paper we investigate the chemistry behind the formation of cluster crystals in zeolites Y and A.

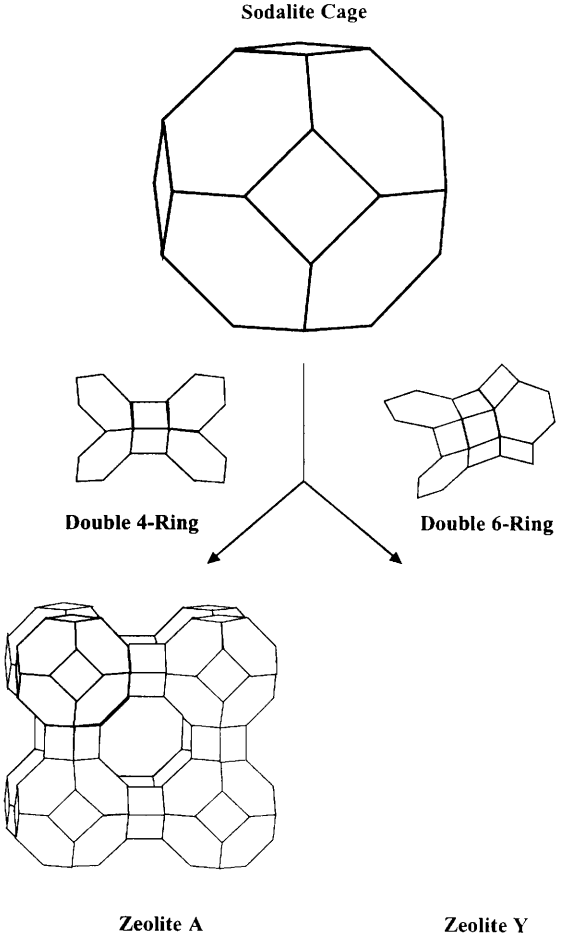

Fig. 1 The framework structure of zeolites A and Y. The vertices of the polyhedra are occupied by silicon or aluminium atoms; the framework oxygens and exchangeable cations are omitted for clarity

† Basis of the presentation given at Dalton Discussion No. 1, 3rd–5th January 1996, University of Southampton, UK.

Non-SI units employed: bar = 10^5 Pa, G = 10^{-4} T, emu = SI × $10^6/4\pi$, eV ≈ 1.60 × 10^{-19} J.

Experimental

Sample preparation

The compounds Na_u/Na_{56}-Y (u = 4, 8, 16, 31, 44 or 64) and K_u/K_{12}-A (u = 0.5, 1, 1.5, 2, 3 or 5) were prepared through the reaction of the dehydrated zeolites Na_{56}-Y ($Na_{56}Al_{56}Si_{136}O_{384}$) and K_{12}-A ($K_{11.5}Al_{11.5}Si_{12.5}O_{48}$) with controlled amounts of metal vapour, corresponding to u atoms per formula unit. The reactions were carried out at 200 °C (Na_{56}-Y) and between 200 and 250 °C (K_{12}-A) in sealed, evacuated quartz reaction tubes as described previously.[1,24] The zeolite Na_{56}-Y was used as received from Laporte Inorganics, while K_{12}-A was prepared from the sodium form (BDH) by standard ion-exchange procedures;[25] near complete exchange was confirmed by atomic absorption and the crystallinity of the resultant material was checked by powder X-ray diffraction.

A suitable amount of zeolite (typically 1–2 g) was placed in a reaction tube heated gradually to 450 °C, and evacuated overnight to better than 10^{-5} mbar. The reaction tube was then taken into a high-quality argon glove-box where high-purity sodium or potassium metal (Aldrich) previously distilled into calibrated capillary tubes[1] was introduced, and returned to the vacuum line to be evacuated and sealed with a gas torch. At no stage did the metal come into contact with the atmosphere. When the sealed tube was later heated the alkali-metal vapour filled the reaction chamber and spontaneous coloration of the zeolite occurred. Careful annealing for up to 72 h resulted in homogeneous products varying from a beautiful burgundy colour (Na_8/Na_{56}-Y) through to jet black (Na_{64}/Na_{56}-Y), and from intense blue (K_1/K_{12}-A) to greenish brown (K_5/K_{12}-A).

ESR and SQUID measurements

A portion of each sample was sealed in the Spectrosil section of the reaction tube so that ESR and magnetic susceptibility measurements could be made without exposing the product to air. First-derivative ESR spectra were recorded on a Bruker ESP 300 spectrometer operating at X-band frequencies (*ca.* 9 GHz) with 100 kHz field modulation. The microwave frequency was measured with a Hewlett-Packard 5350B frequency counter to an accuracy of ± 1 kHz, and the magnetic field with a Bruker ER 035M NMR gaussmeter to better than ± 0.1 G. Temperatures down to 4 K were attained by means of an Oxford Instruments ESR 900 continuous-flow cryostat. The intensity of an ESR signal provides a direct measurement of the paramagnetic susceptibility of the sample. As ESR spectra are normally recorded in first-derivative mode the intensity is obtained through double integration of the recorded spectrum. To quantify these measurements, the intensity from each sample was compared to that of a known $CuSO_4 \cdot 5H_2O$ standard in a dual-mode cavity. Errors in a given measurement are estimated at ± 20% of the absolute value.

Static susceptibilities of two samples were recorded between 4.5 and 50 K on a Cryogenic S100 SQUID magnetometer, with measuring fields of up to 1000 G. Owing to the relatively small moment and sample size the value of the magnetization was found to be relatively small. It was therefore possible to study only the two most paramagnetic samples, and these only below 50 K.

Results

Na_u/Na_{56}-Y

The ESR spectra of Na_u/Na_{56}-Y (u = 4, 8, 16, 31, 44 or 64) recorded at room temperature are shown in Fig. 2. The red solid Na_4/Na_{56}-Y exhibits the characteristic ESR spectrum of Na_4^{3+} paramagnetic clusters, consisting of thirteen equally spaced lines with a hyperfine coupling constant A = 32.7 ± 0.4 G and g = 2.0023 ± 0.0001.[1,26] Also present is a singlet resonance at

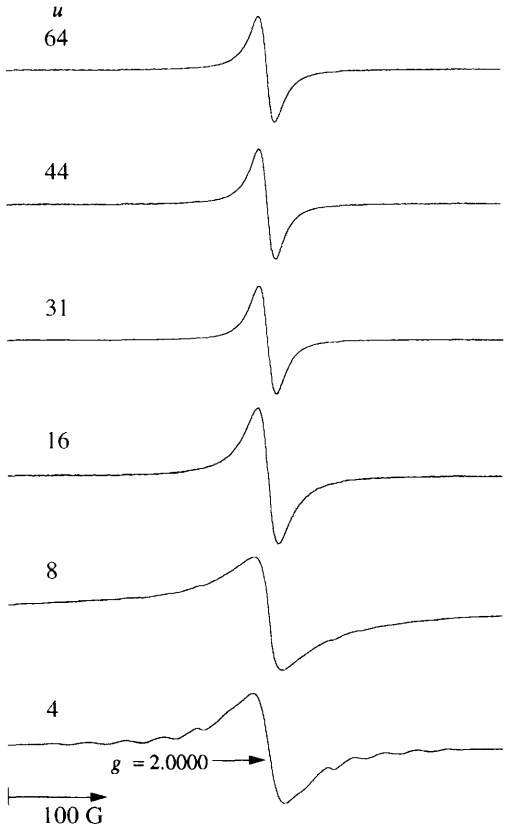

Fig. 2 Room-temperature ESR spectra of Na_u/Na_{56}-Y

g = 2.0013 ± 0.0001, whose relative intensity grows as u increases, and dominates the ESR spectra for u > 8. The first-derivative peak-to-peak linewidths (ΔH_{pp}) for this signal are given in Table 1 and agree well with the results of Anderson and Edwards.[1] The spectra could not be fitted to simple Lorentzian lineshapes; there is more intensity in the wings of the spectra than in a simple Lorentzian. This lineshape is indicative of a composite line, characterized by a distribution of linewidths rather than a single value.[1] Although the measured peak-to-peak linewidth was independent of temperature, the ratio of the intensity in the wings to that in the centre of the resonance grew with rising temperature, suggesting an increase in the relative importance of broader components.

The ESR spin susceptibility at room temperature has been measured for a number of samples. The results are presented in Table 1 along with a summary of the ESR parameters for these compounds. For the purposes of discussion the numbers have been presented in two ways: expressed as a percentage of the value expected for u non-interacting spins (spin fraction), *i.e.* relative to the amount of metal introduced to the zeolite, and relative to the number of sodalite cages in the zeolite (eight per unit cell). The static magnetic susceptibility of Na_8/Na_{56}-Y was recorded at a field of 1000 G, between 4 and 50 K, after the sample had been cooled from room temperature in zero field. The results obtained are plotted in Fig. 3, corrected for the diamagnetism of the atomic cores. The inverse susceptibility plot is shown in Fig. 4, and indicates that the sample obeys a Curie law.

K_u/K_{12}-A

The ESR spectra of K_u/K_{12}-A (u = 0.5, 1, 1.5, 2, 3 or 5) recorded at room temperature are shown in Fig. 5; the ESR parameters of these spectra are summarized in Table 2. The spectra of the two most lightly loaded materials at subambient temperatures are shown in Figs. 6 and 7. It is clear that all of the

Table 1 The ESR parameters for Na_u/Na_{56}-Y

Sample	g (singlet)	ΔH_{pp}/G	% Spin fraction	Spins per sodalite cage
Na_4/Na_{56}-Y	2.0013	32.0	120	0.6
Na_8/Na_{56}-Y	2.0012	27.5	79	0.79
Na_{16}/Na_{56}-Y	2.0011	20.6	50	1.00
Na_{64}/Na_{56}-Y	2.0011	16.1	7	0.6

Table 2 The ESR parameters for K_u/K_{12}-A

Sample	g	ΔH_{pp}/G	% Spin fraction	Spins per sodalite cage
$K_{0.5}/K_{12}$-A	1.9996	2.6	9	0.05
K_1/K_{12}-A	1.9997	complex	25	0.25
$K_{1.5}/K_{12}$-A	1.9987	1.2	35	0.53
	1.9987	6.4		
K_2/K_{12}-A	1.9987	1.4	37	0.74
	1.9979	17		
K_3/K_{12}-A	1.9978	4.2	26	0.78
K_5/K_{12}-A	1.9974	22.0	19	0.95

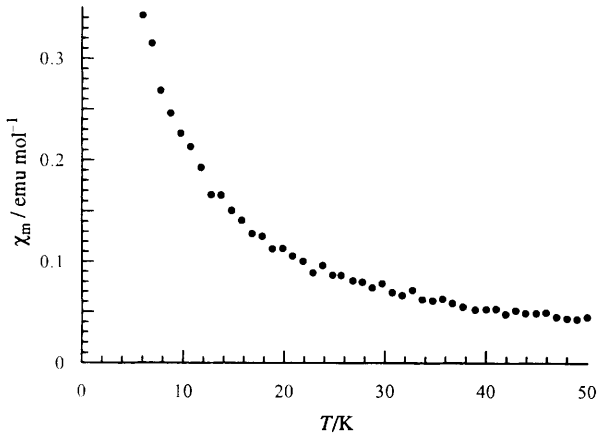

Fig. 3 The molar static magnetic susceptibility of Na_8/Na_{56}-Y as a function of temperature

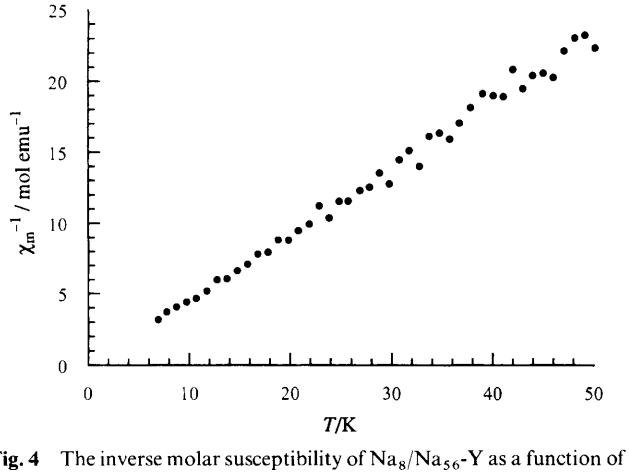

Fig. 4 The inverse molar susceptibility of Na_8/Na_{56}-Y as a function of temperature

compounds studied, with the exception of the most heavily loaded K_5/K_{12}-A, exhibited spectra with at least two components. Cooling the most lightly loaded sample with $u \leqslant 0.5$ to 4 K revealed a weak hyperfine pattern of ten lines ($A \approx 14$ G). At room temperature the spectrum of K_5/K_{12}-A was Lorentzian in shape with a g value of 1.9974 ± 0.0001 and a linewidth of 21.8 ± 0.2 G. This g value was found to be temperature independent, but the linewidth rose with temperature from ≈12 G at 4 K to ≈28 G at 380 K. The

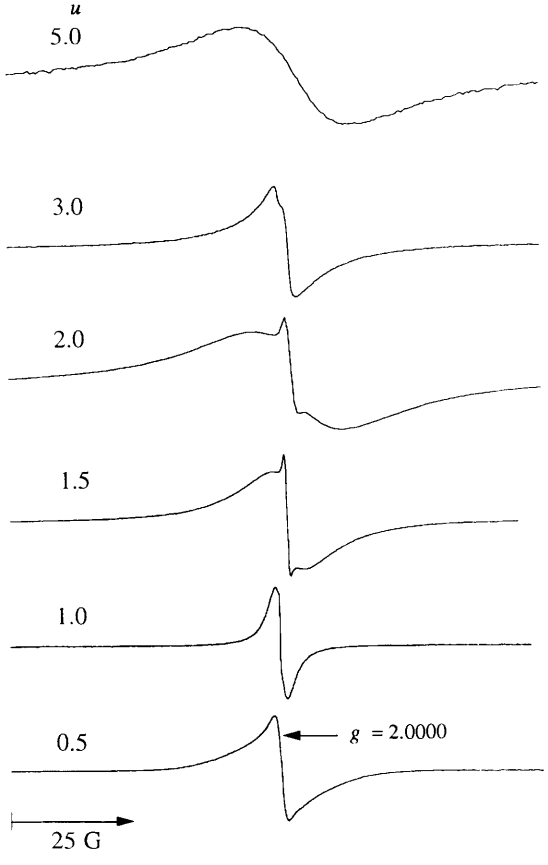

Fig. 5 Room-temperature ESR spectra of K_u/K_{12}-A

absorption lineshape appeared to be Lorentzian over the entire temperature range. The room-temperature ESR spin susceptibility of the samples was also measured; the results are presented in Table 2 in the same format as for Na_u/Na_{56}-Y.

The low-temperature static magnetic susceptibility of K_5/K_{12}-A was recorded at a field of 1000 G, between 4 and 50 K, the sample having been cooled from room temperature in zero field; the results are plotted in Fig. 8 corrected for the diamagnetism of the atomic cores. Two sets of data are presented: first from the 'virgin' sample (fresh from the furnace), and secondly after the sample had been pre-exposed to a magnetic field for 24 h before measurement. A plot of the inverse susceptibility data from the virgin sample can be seen in Fig. 9; again the data follow a Curie law.

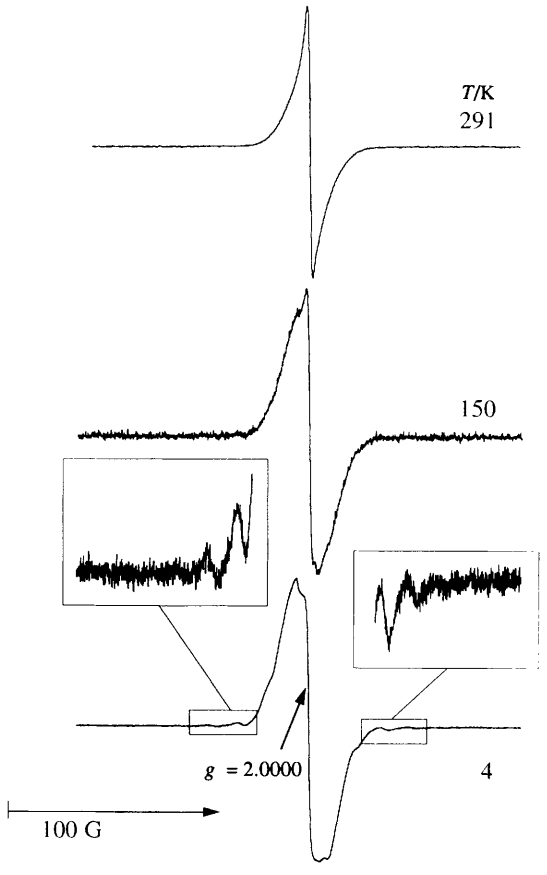

Fig. 6 The ESR spectrum of $K_{0.5}/K_{12}$-A as a function of temperature

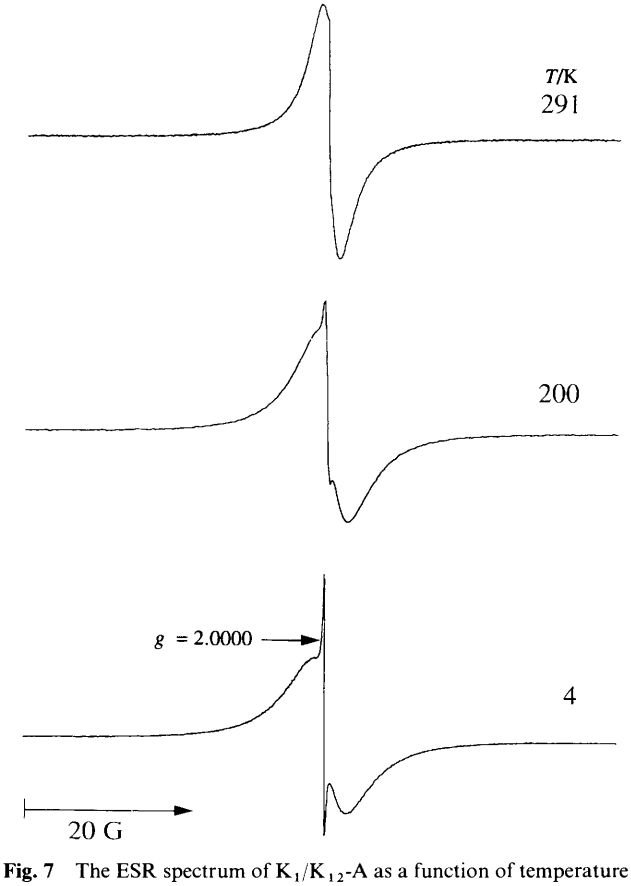

Fig. 7 The ESR spectrum of K_1/K_{12}-A as a function of temperature

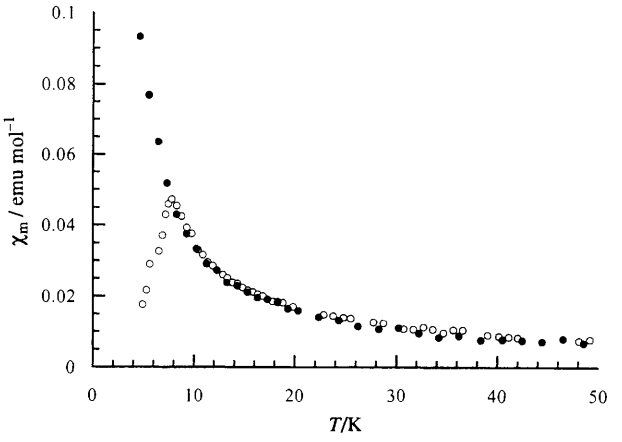

Fig. 8 The molar static magnetic susceptibility of K_5/K_{12}-A as a function of temperature. Open circles show data from a virgin sample (see text), filled circles data from the same sample pre-exposed to a magnetic field for 24 h before measurement

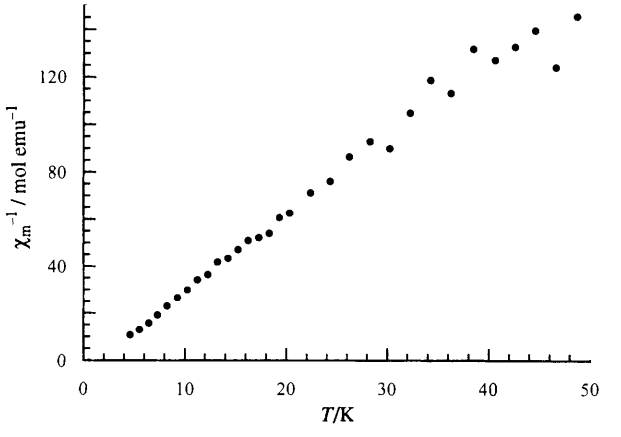

Fig. 9 The inverse molar susceptibility of K_5/K_{12}-A (virgin sample) as a function of temperature

Discussion

Na_u/Na_{56}-Y

Following a series of detailed ESR studies over a number of years the sequence of events occurring when sodium vapour is allowed to interact with dehydrated Na-Y is now qualitatively well known. In the initial stages of reaction the ionization of guest sodium atoms results in the formation of Na_4^{3+} paramagnetic centres comprising an electron trapped amongst four equivalent sodium cations.[1,17,18] This Na_4^{3+} cluster was first observed by Kasai[26] on irradiation of dehydrated Na-Y with γ- or X-rays under vacuum.

Two possible locations have been proposed for the Na_4^{3+} cluster in zeolite Y: the observation of nearly identical ESR spectra in sodium-loaded zeolites Y and A, and in the mineral sodalite, was regarded by Edwards and co-workers[18] as strong evidence that Na_4^{3+} was located in the sodalite cage (β cage) structural unit, common to all three hosts; Liu and Thomas,[27] on finding that the introduction of toluene (too large to enter the sodalite cage) to γ-irradiated zeolites X and Y caused the disappearance of the UV/VIS absorption band attributed to Na_4^{3+}, have argued that the cluster resides in the larger supercage, as originally proposed by Kasai.[26] Using powder neutron diffraction data we have recently completed the Rietveld refinement of the structure of the sample of nominal concentration Na_8/Na_{56}-Y,[28] which revealed a large net movement of sodium cations into the sodalite cage to form Na_4^{3+} clusters. For this sample the refinement was consistent with a 73% occupancy of the sodalite cages with Na_4^{3+} clusters.

Static susceptibility measurements performed on the SQUID magnetometer record the total susceptibility of the sample χ_{tot}, which is related to the ESR spin susceptibility $\chi^{\varepsilon}_{para}$ through the relation (1), where $\chi^{\varepsilon}_{para}$ and χ^{ε}_{dia} are the paramagnetic and

$$\chi_{tot} = \chi^{\varepsilon}_{para} + \chi^{\varepsilon}_{dia} + \chi^{co}_{dia} \quad (1)$$

diamagnetic contributions respectively to the electronic susceptibility, and χ^{co}_{dia} is the diamagnetism of the atomic cores. The latter contribution is normally subtracted to leave the experimental electronic susceptibility as presented in Figs. 3 and 4 for Na_8/Na_{56}-Y. The Curie-law behaviour observed indicates that this is dominated by the paramagnetic contribution and enables us to determine the ratio $\chi_{exptl}/\chi_{theory}$ at each temperature, where χ_{exptl} is the experimentally determined molar susceptibility, corrected for core diamagnetism, and χ_{theory} is the theoretical value of the molar susceptibility, assuming that the sample is behaving as an ideal Curie paramagnet. For x mol of non-interacting spins, the Curie spin susceptibility (in cgs units) is given by equation (2).

$$\chi_{theory} \approx 3x/8T \quad (2)$$

The ratio $\chi_{exptl}/\chi_{theory}$ is known as the spin fraction and is commonly expressed as a percentage.

For Na_8/Na_{56}-Y the spin fraction, as defined above, was found to be $\approx 74 \pm 4\%$ over the temperature range of the experiment, in excellent agreement with the crystallographic data. Together these measurements are fully consistent with the presence of Na_4^{3+} clusters in around three quarters of the sodalite cages of Na_8/Na_{56}-Y. Despite this high concentration of Na_4^{3+}, the characteristic 13-line pattern is only weakly present in the ESR spectrum of this compound (Fig. 2), and even at this relatively modest concentration of metal the dominant feature is a symmetric singlet. This line, which is also observed for the darker, more concentrated solids resulting from the incorporation of larger amounts of sodium (Fig. 2), was formerly attributed to the formation of metallic clusters within the zeolite pores.[10]

Significantly, the refined structure of Na_8/Na_{56}-Y provides no evidence for the presence of a second cluster.[28] This observation accords with recent work casting doubt on the established interpretation,[10] and it has been proposed that the ESR line in fact results from the interaction of localized unpaired electrons in neighbouring Na_4^{3+} clusters,[1] which may be sufficiently close to one another that their wavefunctions overlap and they are coupled through quantum-mechanical exchange forces. The observed[28] distance through the hexagonal prisms between sodium atoms in Na_4^{3+} clusters in neighbouring sodalite cages is only 5.36 Å, short enough to explain the loss of the ESR hyperfine structure at modest metal loadings. Ursenbach *et al.*[11] have estimated the exchange interaction of nearest-neighbour paramagnetic Na_4^{3+} clusters at *ca.* 8×10^{-7} eV. This value is comparable to the inverse of the observed ^{23}Na hyperfine coupling constant for Na_4^{3+}. We would therefore expect to see a collapse of the hyperfine structure at concentrations where each cluster had at least one cluster neighbour, and the hyperfine structure will be observed only from isolated clusters. Although interactions of the magnitude mentioned above are sufficient to wash out the fingerprint hyperfine splitting pattern of Na_4^{3+}, they are much too small to have any significant effect on the observed magnetic susceptibility of the sample.[11]

In Na_8/Na_{56}-Y a three-dimensional network of interacting Na_4^{3+} clusters, located in the sodalite cages, is clearly the source of the controversial ESR line. These clusters, whose distances from and orientations relative to each other are fixed by the zeolite host, constitute a cluster crystal (Fig. 10), whose order is broken only by the fact that a proportion of the cages

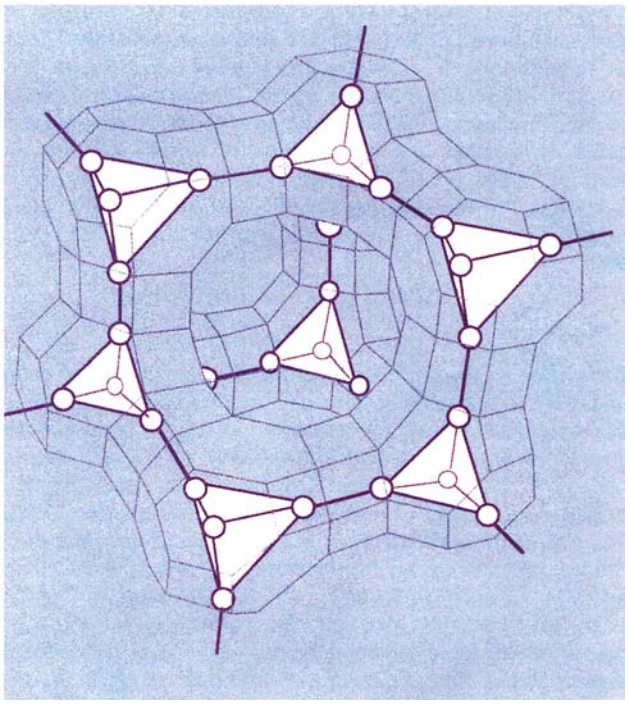

Fig. 10 Representation of a cluster crystal composed of interacting Na_4^{3+} clusters in zeolite Y

remains empty. In theory a nominal sodium metal concentration of $u = 8$ is sufficient to place an Na_4^{3+} unit in each sodalite cage and form a perfect cluster crystal, whose formation may be written as in equation (3) where Z_Y^{56-} represents the anionic

$$8Na^0 + (Na^+)_{56}Z_Y^{56-} \longrightarrow (Na^+)_{32}(Na_4^{3+})_8Z_Y^{56-} \quad (3)$$

framework of zeolite Y. The incompleteness of the cluster array is largely explained by the crystallographically determined composition of this compound which was closer to Na_7/Na_{56}-Y or $(Na^+)_{35}(Na_4^{3+})_7Z_Y^{56-}$.[28] The inevitable slight uncertainty in sample composition,[1] a problem which is particularly acute when dealing with low concentrations, plausibly also accounts for the enhanced ESR spin susceptibility of Na_4/Na_{56}-Y (Table 1).

Molecular dynamics simulations by Ursenbach *et al.*[11] identify Na_4^{3+} as comfortably the most stable electron trap in Na-Y. The growth of the perfect cluster crystal (Fig. 10) therefore requires only a sodium metal concentration $u \geqslant 8$. The presence of such a crystal in Na_{16}/Na_{56}-Y may be inferred from ESR spin-susceptibility measurements (Table 1), which show a moment for this compound equivalent to one Na_4^{3+} cluster per sodalite cage. This conclusion is confirmed by the preliminary results of neutron diffraction studies on this compound.[29] Remaining electrons released from the ionization of sodium atoms entering the zeolite, over and above the eight located in Na_4^{3+} traps within the sodalite cages, apparently do not contribute significantly to the paramagnetism of the sample. This finding may be compared to the results of Ursenbach *et al.*,[11] who also note a strong tendency towards spin pairing in clusters formed in the supercages after the filling of the sodalite cages is complete.

The importance of electron spin pairing in these compounds is confirmed by the ESR spin susceptibility of Na_{64}/Na_{56}-Y (Table 1), where only $\approx 7\%$ of electron spins remain unpaired and contribute to the paramagnetic susceptibility. Similar low spin fractions have also been observed in caesium-loaded zeolite A,[30] and are reminiscent of the behaviour seen in, for example, concentrated metal–ammonia solutions,[31] where the majority

of the excess of electrons are also spin-paired. Interestingly, the observed moment of Na_{64}/Na_{56}-Y is equivalent to only 0.6 spin per sodalite cage. It is not yet clear to what extent this reduced susceptibility results from much stronger interactions between the Na_4^{3+} clusters, mediated perhaps by electrons residing in diamagnetic states in the supercage, or simply indicates the eventual break up of the cluster crystal, caused either by ionization into the supercage network of electrons previously trapped (as Na_4^{3+}) or by degradation of the zeolite crystal itself.

K_u/K_{12}-A

In contrast to the sodium in zeolite Y system, interest in the potassium in zeolite A system has been comparatively recent. An early ESR study by Anderson *et al.*[19a] identified the presence of K_3^{2+} clusters at low values of u. Terasaki and co-workers[2,3] have since examined the optical and magnetic properties of a range of more concentrated samples and found evidence of itinerant electron ferromagnetism and re-entrant spin glass behaviour, while structural studies have been carried out by Seff and co-workers[15,32] and Armstrong *et al.*[24,33] The latter have recently detailed the formation of a unique superlattice in the compound K_5/K_{12}-A, where each sodalite cage contains four potassiums separated by 4.72 Å, and alternating α cages contain twelve and eight potassiums.[24,33]

Detailed analysis of the available crystallographic data suggests that the four potassium ions in the sodalite cage may constitute a K_4^{3+} cluster, analogous to the Na_4^{3+} and K_4^{3+} clusters observed in zeolite Y,[17,18] which also contains the sodalite cage structural unit. Certainly, it seems unlikely that four potassium ions would happily squeeze into the sodalite cage without some excess of electron density to alleviate cation–cation repulsions. Significantly the sodalite cage contains no potassium cations in dehydrated K_{12}-A.[24] Fig. 11 shows the maximum possible occupancy of the sodalite cage with K_4^{3+} clusters (inferred from crystallographic data)[24] in a number of K_u/K_{12}-A samples, plotted alongside the ESR spin susceptibilities measured in spins per sodalite cage (Table 2). There is a noticeable correlation between these two sets of data over a range of concentrations. This is particularly striking when one considers that one formula unit of K_{12}-A contains only one sodalite cage, and that the incorporation of one potassium atom per formula unit could conceivably produce a paramagnetic moment equivalent to one electron per sodalite cage.

Over the range of concentrations the data in Fig. 11 are consistent with the suggestion that we are observing only those excess electrons associated with K_4^{3+} (or K_3^{2+}) clusters in the sodalite cages. In K_5/K_{12}-A five electrons are introduced per formula unit. The observed spin fraction, at $\approx 20\%$, accounts for a K_4^{3+} cluster in each sodalite cage, with the other $\approx 80\%$ of excess electrons, as in the case of Na_u/Na_{56}-Y, residing in spin-paired states in the larger cages. In the case of zeolite A these larger cages are the α cages, and we have seen that in K_5/K_{12}-A they host two very different arrangements of potassium cations, containing alternately twelve and eight potassium ions in a perfectly ordered superlattice.[24,33] Half the α cages thus retain the structure of dehydrated K_{12}-A, while the rest are much more tightly packed, and logic and crystallographic evidence[24,33] dictates that it is in the latter where the remaining electrons are to be found. The suggestion that potassium ions bearing significant excess of electron density might coexist, in close proximity, with others bearing none is supported by the simulations of Ursenbach *et al.*,[11] which found that the effective electron affinity of sodium cations in the supercage six-ring site in Na_u/Na_{56}-Y was very low. The potassium ions thought to bear little or no excess of electron density in K_5/K_{12}-A occupy an equivalent six-ring site in the α cage of zeolite A. The crystallographic and susceptibility data are therefore consistent with the formulation of K_5/K_{12}-A as a cluster crystal

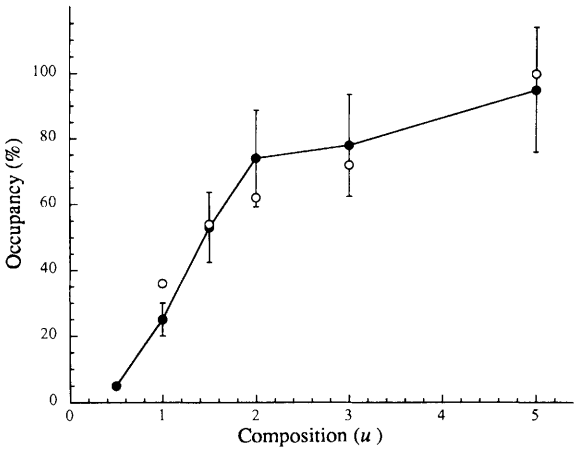

Fig. 11 The maximum percentage occupancy of the sodalite cage in K_u/K_{12}-A with K_4^{3+} clusters inferred from ESR spin-susceptibility measurements (●) and crystallographic data (○) (see ref. 24)

$(K^+)_{14}(K_4^{3+})_2K_{12}^{4+}Z_A^{24-}$ containing paramagnetic K_4^{3+} and diamagnetic K_{12}^{4+} clusters (Fig. 12).

As was the case in Na_u/Na_{56}-Y, the large concentration of K_4^{3+} clusters in the sodalite cages is not directly reflected in the ESR spectra of K_u/K_{12}-A: none of the samples exhibits the characteristic hyperfine splitting pattern observed from K_4^{3+} clusters in zeolite Y. Furthermore, the weak hyperfine pattern of ten lines observed on cooling the most lightly loaded sample to 4 K (Fig. 6) implies the presence of K_3^{2+} rather than K_4^{3+}. The observed spin fraction of $\approx 10\%$ (Table 2), equivalent to one spin per twenty sodalite cages, is the lowest for K_u/K_{12}-A and may reflect the comparative instability of K_3^{2+}. This concentration $u \approx 0.5$, enough in theory to half fill the sodalite cage with clusters, is directly comparable to the concentration $u = 4$ in Na_u/Na_{56}-Y, and the observation that even at this low concentration over 90% of the excess electrons reside in diamagnetic states is in direct contrast to the case of sodium in zeolite Y.

The absence of any hyperfine splitting in any of the more concentrated K_u/K_{12}-A samples is unsurprising. Even for K_1/K_{12}-A the ESR spin-susceptibility results indicate that around a quarter of the sodalite cages may be occupied with K_4^{3+} (or K_3^{2+}) clusters. This occupancy is such that hyperfine splittings will be lost if clusters in neighbouring cages interact with each other as in Na_u/Na_{56}-Y. In fact the geometry of zeolite A is such that, even allowing for the fact that the wavefunctions of electrons in potassium clusters may well extend further than in the sodium case, direct interactions between the clusters are less likely. This is because in contrast to zeolite Y, where the atoms of neighbouring Na_4^{3+} clusters directly face each other through the hexagonal prisms which link the sodalite cages (Fig. 1), the sodalite cages in zeolite A are connected through small cubes, and the ions of sodalite cage clusters instead face into the α cages.

In the case of K_u/K_{12}-A it is probable that the interactions between sodalite cage clusters responsible for the absence of hyperfine splitting are mediated through electrons in diamagnetic states in the α cages. Such interactions are also implicated in the spin-glass-like history-dependent magnetic behaviour exhibited by K_5/K_{12}-A (Fig. 8), which can result in the observation of extremely small magnetic moments at low temperature. The g values of the singlet ESR lines in K_u/K_{12}-A (Table 2) are comparable to those for bulk and particulate potassium metal, and are consistently lower than those for the sodium system, reflecting the larger spin–orbit coupling of potassium. The lineshape is found to be Lorentzian over the entire temperature range studied, suggesting the absence of the linewidth distribution which characterizes Na_u/Na_{56}-Y, but all of the compounds studied, with the exception of the most

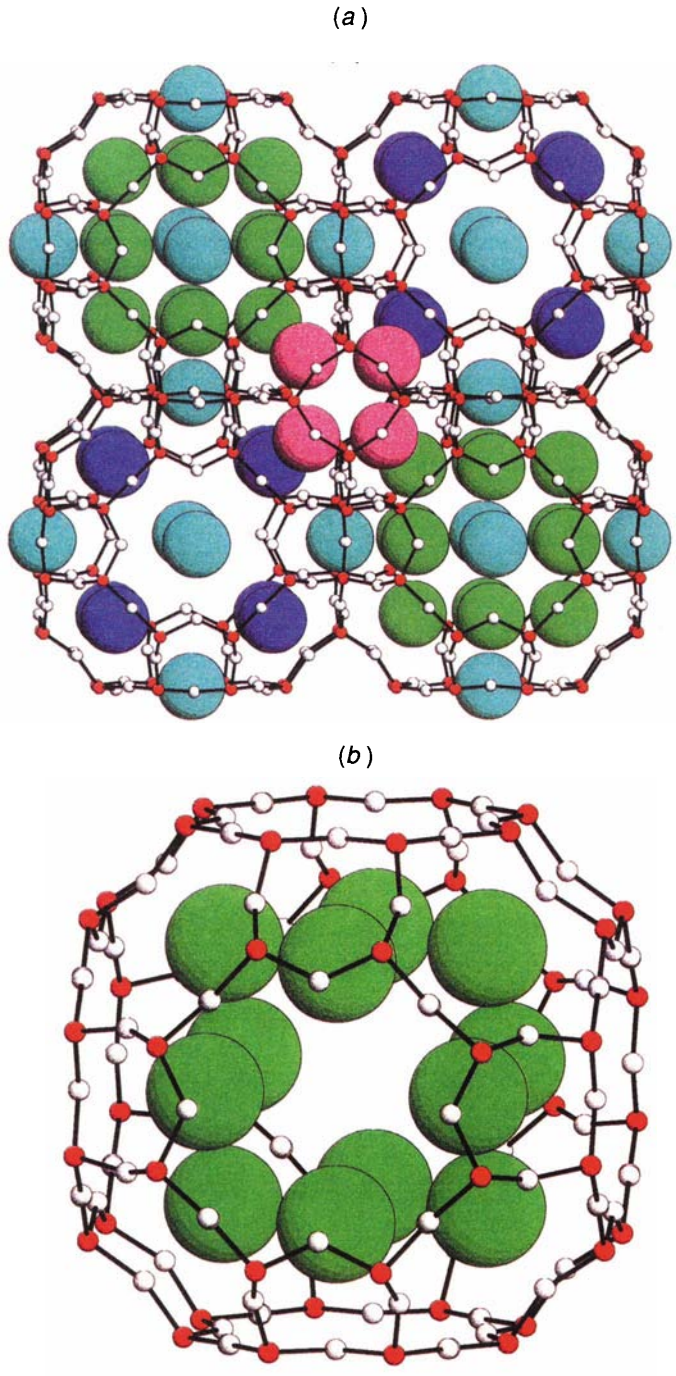

Fig. 12 (*a*) The structure of K_5/K_{12}-A showing a cluster crystal composed of sodalite cage K_4^{3+} clusters (pink) and α-cage K_{12}^{4+} clusters (green). Also shown are the eight-ring (turquoise) and the six-ring (blue) potassium ions. (*b*) Structure of the K_{12}^{4+} cluster

heavily loaded K_5/K_{12}-A, did exhibit spectra with at least two components. The absence of the narrower component (which accounts for a relatively small proportion of the observed ESR intensity) in the spectrum of the perfect cluster crystal K_5/K_{12}-A suggests that this may arise from some arrangement of ions and electrons which might be regarded as a defect in the cluster crystal caused by incomplete long-range ordering.

Critique of the cluster crystal model

The term cluster enjoys a wide currency in physics and chemistry to describe many different types of groupings of atoms or molecules held together by a variety of interactions. These range from chemical bonds to the much weaker interactions found for example in gaseous rare-gas clusters. In the inorganic chemistry domain a metal atom cluster has been classically defined as a group of two or more metal atoms in which there are substantial and direct bonds between the metal atoms. The question as to what extent alkali-metal clusters in zeolites meet this definition was first addressed by Anderson and Edwards,[19b] who compared the hyperfine splitting of a series of zeolite-based $Na_n^{(n-1)+}$ clusters with a range of neutral and charged sodium and silver clusters, to conclude that the valence electron in clusters such as Na_4^{3+} remains rather loosely associated with the cations. The implication of this work was that the zeolite-based species are best regarded not as tightly bound molecular clusters entrapped within the host but as electron traps akin to F centres in crystalline salts.

The preceding paragraph advances the picture of alkali-metal clusters in zeolites as comprising a number of cations co-ordinated to the walls of a zeolite cage with electrons occupying the cavity space, a scenario which is fully justified by the geometry of the ions in the three clusters considered in this work. The comparison between an electron in clusters such as Na_4^{3+} and K_4^{3+} occupying the cavity space of the sodalite cage and an electron trapped within solvent cavities in, for example, liquid ammonia has already been noted. The striking 'hollow' arrangement of the K_{12}^{4+} cluster [Fig. 12(*b*)] suggests that the pattern described extends also to this much larger multielectron cluster.

Of all the alkali-metal clusters known in zeolites, Na_4^{3+} is amongst the most stable. In Na-Y it has been found to remain intact up to and beyond 500 °C, to exhibit a spectrum which was practically unchanged between room temperature and 4 K, and to be present in deliberately overheated samples long after other resonances and long-range crystallographic order had disappeared.[1,34] This apparent stability belies the fact that calculations on gas-phase Na_4^{3+} predict only a shallow minimum.[35] (It is worth recalling that a tetrahedral cluster of four atoms requires six bonds to hold it together, implying a bond order of one twelfth if this feat is accomplished by just one electron.) The key to the stability of Na_4^{3+} in zeolites lies in the observations that it occurs only in zeolites containing the sodalite cage structural unit, and that the four ions forming the cluster are located in normal zeolite cation sites.[28] Clearly the formation of Na_4^{3+} owes as much to the co-ordination of the cations to the zeolite framework as to the binding power of the single excess electron.

Whatever the strength of the bonding between sodium ions in Na_4^{3+}, the cluster, as we have seen, is sufficiently stable that the reaction of sodium vapour with dehydrated Na-Y results in zeolite cations being drawn into the sodalite cage to form Na_4^{3+} clusters, and indeed exclusively in the formation of Na_4^{3+}, until the sodalite cages are filled.[11,28] The same cannot be said of the clusters in K_u/K_{12}-A. At compositions up to $u = 1$, enough in theory to form a K_4^{3+} (or K_3^{2+}) in each sodalite cage, it is clear that in fact only a minority of cages contain such a cluster, and the sodalite cages are eventually completely filled with K_4^{3+} only at five times this concentration.

To understand fully the zeolite crystal chemistry involved in cluster formation in the K_u/K_{12}-A system it is instructive to consider how the distribution of cations changes as extra potassium is introduced. In dehydrated K_{12}-A[24] potassium cations essentially occupy two main co-ordination sites, a six-ring α-cage site [blue in Fig. 12(*a*)] and an eight-ring site between the α cages (turquoise), both of which are filled. The arrival from the vapour phase of extra potassium into the zeolite thus presents a problem, which is initially solved through the entry of cations into the sodalite cage which is scarcely occupied in dehydrated K_{12}-A. The number of cations required to occupy the sodalite cage mounts quite quickly as extra potassium enters the zeolite: if a cation in the favoured six-ring α-cage site moves into the sodalite cage it remains too close to its original site for that to be occupied by the incoming atom. It

requires at least *two* neighbouring ions to make this move to release a new four-ring site (green) between them. It may therefore be no coincidence that the sodalite cages of K_1/K_{12}-A contain on average approximately two potassium ions.[24]

The cation repulsions that inevitably result from the presence of two or more potassium ions (pink) within the sodalite cage can be alleviated by the trapping of excess electrons in K_3^{2+} and K_4^{3+} clusters. The sample K_1/K_{12}-A with an average of two potassiums per sodalite cage may well contain a number of K_3^{2+} and K_4^{3+} clusters with a corresponding number of sodalite cages containing only one potassium cation. This goes some way towards explaining why the crystallographic occupancy of the sodalite cage is observed to be greater than that inferred from ESR susceptibility data at this composition (Fig. 11). Crystallographic evidence[24] also points to a considerable degree of mobility amongst the sodalite cage cations at room temperature in this compound, but as we shall see this echo of the kind of fluidity described by Ursenbach *et al.*[11] in Na_u/Na_{56}-Y disappears as zeolite A fills up with potassium ions.

The gradual net displacement of cations from six-ring sites of which there are up to eight in each α cage into the four-ring sites of which there are twelve also helps accommodate more potassium ions, and this process proceeds much more efficiently if six-ring sites are progressively vacated next to already empty sites. It is this contingency that predisposes the zeolite cations towards the ordering and cluster formation observed in K_u/K_{12}-A. The tendency for cations in the two α-cage sites to divide into separate α cages, and the consequent closeness of the four-ring site cations to those occupying the eight-ring sites between neighbouring α cages and to each other, is facilitated, as in the sodalite cage, by the presence of excess electrons. Ultimately in K_5/K_{12}-A this results in the ordered cluster crystal described earlier (Fig. 12), but it is possible, indeed likely, that with compositions containing less potassium other clusters may be formed, including those that might be regarded as fragments of the K_{12}^{4+} unit.

By now it is clear that the clustering phenomenon observed in alkali-metal zeolites is dictated by the zeolite framework and the collective co-ordination chemistry of the zeolite cations rather than the strength of the bonding between metal atoms. Indeed Ursenbach *et al.*[11] have found that stable clusters are formed in the supercages of zeolite Y only if anchored to the framework through one or more co-ordinated cations. Although it is difficult to think of Na_8/Na_{56}-Y in anything other than cluster terms the situation for K_5/K_{12}-A is nowhere near so clear cut. In choosing to formulate this compound as a cluster crystal containing K_4^{3+} and K_{12}^{4+} it is important not to lose sight of the fact that no potassium ion in the structure is more than 4.9 Å away from its nearest neighbours.[24] This compares with a potassium–potassium distance within the K_4^{3+} clusters of 4.719 Å, and justifies the description of Sun and Seff[15] of a cationic continuum in the K_u/K_{12}-A system. Equally, if the rather short distance of 4.436 Å between the cations which comprise K_{12}^{4+} is taken as good evidence for the existence of this cluster, then the even shorter distance of 4.238 Å between these and the eight-ring site cations lends weight to the suggestion that K_{12}^{4+} might equally well be regarded as K_{18}^{10+}. For the moment the extent to which the eight-ring site cations bear an excess of electron density remains hard to quantify. Simulations suggest that such highly charged clusters are not favoured, in Na_u/Na_{56}-Y at least.[11]

Whatever the ambiguities in formulation, there are still strong pragmatic grounds for considering compounds such as K_5/K_{12}-A within the cluster model. Theoretical studies suggest that the excess of electrons released when alkali-metal atoms enter a dehydrated zeolite do not, in the ground state at least, interact to any great extent with the aluminosilicate framework, but remain associated with the zeolite cations, and it is the excess electron states that largely determine the electronic and magnetic properties of these compounds. It is perhaps only by considering such materials as ordered arrays of closely packed, interacting clusters that we can hope to model the essential heterogeneity at the nanoscale level that is a vital determinant of their overall electronic and magnetic properties.

An example of the power of this model in action lies in the recent work of Nozue and co-workers,[2,3,5] who treated alkali-metal-loaded zeolite A as a cluster crystal composed of interacting α-cage clusters, the clusters themselves being modelled by assuming the excess of electrons experience a spherical potential furnished by the cations within the α cage. This model, analogous to the jellium model for gas-phase alkali-metal clusters, has been successfully applied to interpret both the ferromagnetism and optical properties observed in a number of compounds including K_u/K_{12}-A. Although we have not ourselves observed ferromagnetism in the K_u/K_{12}-A system, it is interesting that with the eight excess electrons completely filling the 1s and 1p levels of the spherical potential well the model predicts that K_{12}^{4+} (or K_{18}^{10+}) should be diamagnetic, as we have observed, and may even display enhanced stability on account of its shell-filling 'magic' number of eight electrons. We anticipate that cluster-based models will prove increasingly useful in rationalizing the unusual electronic and magnetic properties of a wide range of similar compounds.

Acknowledgements

We would like to thank the EPSRC for support and provision of neutron beam facilities. P. A. A. is a Royal Society Research Fellow.

References

1 P. A. Anderson and P. P. Edwards, *J. Am. Chem. Soc.*, 1992, **114**, 10 608.
2 Y. Nozue, T. Kodaira and T. Goto, *Phys. Rev. Lett.*, 1992, **68**, 3789.
3 T. Kodaira, Y. Nozue, S. Ohwashi, T. Goto and O. Terasaki, *Phys. Rev. B*, 1993, **48**, 12 245; Y. Nozue, T. Kodaira, S. Ohwashi, T. Goto and O. Terasaki, *Phys. Rev. B*, 1993, **48**, 12 253.
4 P. A. Anderson, A. R. Armstrong and P. P. Edwards, *Angew. Chem.*, 1994, **106**, 669; *Angew. Chem., Int. Ed. Engl.*, 1994, **33**, 641.
5 Y. Nozue, T. Kodaira, S. Ohwashi, N. Togashi, T. Monji and O. Terasaki, *Stud. Surf. Sci. Catal.*, 1994, **84**, 837.
6 M. J. Kelly, *J. Phys. Condensed Matter*, 1995, **7**, 5507.
7 V. I. Srdanov, K. Haug, H. Metiu and G. D. Stucky, *J. Phys. Chem.*, 1992, **96**, 9039.
8 P. P. Edwards, L. J. Woodall, P. A. Anderson, A. R. Armstrong and M. Slaski, *Chem. Soc. Rev.*, 1993, **22**, 305.
9 A. Monnier, V. I. Srdanov, G. D. Stucky and H. Metiu, *J. Chem. Phys.*, 1994, **100**, 6944.
10 P. A. Anderson and P. P. Edwards, *Phys. Rev. B*, 1994, **50**, 7155.
11 C. P. Ursenbach, P. A. Madden, I. Stich and M. C. Payne, *J. Phys. Chem.*, 1995, **99**, 6697.
12 P. A. Anderson, L. J. Woodall, A. Porch, A. R. Armstrong, I. Hussain and P. P. Edwards, *Mater. Res. Soc. Proc.*, in the press.
13 P. P. Edwards, P. A. Anderson and J. M. Thomas, *Acc. Chem. Res.*, in the press.
14 T. Sun, K. Seff, N. H. Heo and V. P. Petranovskii, *Science*, 1993, **259**, 495; *J. Phys. Chem.*, 1994, **98**, 5768.
15 T. Sun and K. Seff, *J. Phys. Chem.*, 1993, **97**, 5213, 10 756.
16 J. L. Dye, *Prog. Inorg. Chem.*, 1984, **32**, 327.
17 J. A. Rabo, C. L. Angell, P. H. Kasai and V. Schomaker, *Discuss. Faraday Soc.*, 1966, **41**, 328.
18 P. P. Edwards, M. R. Harrison, J. Klinowski, S. Ramdas, J. M. Thomas, D. C. Johnson and C. J. Page, *J. Chem. Soc., Chem. Commun.*, 1984, 982; M. R. Harrison, P. P. Edwards, J. Klinowski, J. M. Thomas, D. C. Johnson and C. J. Page, *J. Solid State Chem.*, 1984, **54**, 330.
19 (*a*) P. A. Anderson, R. J. Singer and P. P. Edwards, *J. Chem. Soc., Chem. Commun.*, 1991, 914; (*b*) P. A. Anderson and P. P. Edwards, *J. Chem. Soc., Chem. Commun.*, 1991, 915.
20 B. Xu and L. Kevan, *J. Chem. Soc., Faraday Trans.*, 1991, 2843.
21 P. A. Anderson, D. Barr and P. P. Edwards, *Angew. Chem.*, 1991, **103**, 1511; *Angew. Chem., Int. Ed. Engl.*, 1991, **30**, 1501.

22 N. H. Heo and K. Seff, *J. Am. Chem. Soc.*, 1987, **109**, 7986; S. H. Song, Y. Kim and K. Seff, *J. Phys. Chem.*, 1991, **95**, 9919; Y. Kim, Y. W. Han and K. Seff, *J. Phys. Chem.*, 1993, **97**, 12 663.
23 V. N. Bogomolov, *Usp. Fiz. Nauk.*, 1978, **124**, 171; *Sov. Phys.-Usp.*, 1978, **21**, 77.
24 A. R. Armstrong, P. A. Anderson and P. P. Edwards, *J. Solid State Chem.*, 1994, **111**, 178.
25 H. S. Sherry, *J. Phys. Chem.*, 1966, **70**, 1158.
26 P. H. Kasai, *J. Chem. Phys.*, 1965, **43**, 3322.
27 X. Liu and J. K. Thomas, *Langmuir*, 1992, **8**, 1750.
28 A. R. Armstrong, P. A. Anderson, L. J. Woodall and P. P. Edwards, *J. Am. Chem. Soc.*, 1995, **117**, 9087.
29 A. R. Armstrong, P. A. Anderson, L. J. Woodall and P. P. Edwards, unpublished work.
30 A. R. Armstrong, P. A. Anderson, L. J. Woodall and P. P. Edwards, *J. Phys. Chem.*, 1994, **98**, 9279.
31 P. P. Edwards, in *Physics and Chemistry of Electrons and Ions in Condensed Matter*, eds. J. V. Acrivos, N. F. Mott and A. D. Yoffe, NATO ASI Ser., D. Reidel, Dordrecht, 1984, vol. 130, pp. 297–333.
32 T. Sun and K. Seff, *J. Phys. Chem.*, 1994, **98**, 10156.
33 A. R. Armstrong, P. A. Anderson and P. P. Edwards, *J. Chem Soc., Chem. Commun.*, 1994, 473.
34 P. H. Kasai and R. J. Bishop, *J. Phys. Chem.*, 1973, **77**, 2306.
35 P. Sen, C. N. R. Rao and J. M. Thomas, *J. Mol. Struct.*, 1986, **146**, 171.

Received 18*th September* 1995; *Paper* 5/06724C